

Structural and Bonding Trends in Ruthenium Pyrochlores

B. J. Kennedy

School of Chemistry, The University of Sydney, Sydney, New South Wales 2006, Australia

and

T. Vogt

Physics Department, Building 510B, Brookhaven National Laboratory, Upton, New York 11973

Received November 13, 1995; in revised form June 17, 1996; accepted June 26, 1996

The structures of four semiconducting ruthenium pyrochlores, $Ln_2Ru_2O_7$ ($Ln = Pr, Nd, Tb, \text{ and } Yb$) have been determined by Rietveld refinement of powder neutron diffraction data. These structures, when compared with those of other Ru containing pyrochlores, especially the metallically conducting pyrochlores, demonstrate that the differences in the Ru–O bond distances between metallic and semiconducting ruthenium pyrochlores are small and highlight the importance of the easily polarizable group 13/15 cations in facilitating large Ru–O–Ru angles. While Ru–O–Ru angles greater than 133° are undoubtedly necessary to facilitate metallic conductivity, it appears that electron delocalization from the A site cation is at least equally important. © 1996 Academic Press, Inc.

INTRODUCTION

The pyrochlore structure was first determined by von Gaertner in 1930 (1) and over the following 65 years many hundreds of pyrochlore type materials have been characterized. Most of the earlier studies were the topic of a comprehensive review by Subramanian *et al.* in 1983 (2). During the past 15 years there has been considerable growth in the number of reported studies on pyrochlore-type oxides as a consequence of the stability and diverse physical properties of these materials. The pyrochlore structure with general formula $A_2B_2O_6O'$ is formed by a wide variety of ions and tolerates a high degree of nonstoichiometry on the O' anion and the A cation sites (2). The ideal pyrochlore structure, space group $Fd\bar{3}m$ (No 277), has eight formula units per cell; see Fig. 1. Depending on the study the origin can be chosen for either the A or the B cation. Typically for ruthenate pyrochlores (3–6) the origin is chosen such that the larger A cations occupy the 16(c) sites at (0.5, 0.5, 0.5) and have a compressed MO_8 scalenohedral coordination. The smaller B cations, in the 16(d) sites at (0, 0, 0), are bonded to six anions at equal

distances, forming a trigonal antiprism with an octahedron as the limiting case. The oxygen anions, O and O' , often labeled O(1) and O(2), occupy the 48(f) ($x, 1/8, 1/8$) and 8(b) ($3/8, 3/8, 3/8$) sites, respectively. Thus, in order to completely describe the three-dimensional arrangement of ions in the structure, only one positional parameter must be determined. In principle the unknown oxygen coordinate can be determined by both X-ray and neutron diffraction; however, the relatively small X-ray scattering power of oxygen compared to the lanthanides (Ln) or transition metals suggests that neutron diffraction is the more appropriate technique, especially when only powder samples are available.

The ruthenate pyrochlores are among the most widely studied pyrochlores due to both their technological importance, as electrode materials (7), catalysts (8, 9), and components in thick film resistors (10), and their unusual electronic properties (11–13); the Ru 4d electrons are borderline between localized and itinerant behavior and depending on the A-type cation the materials are either metallic Pauli paramagnets, e.g., $Bi_2Ru_2O_{7-y}$, or semiconductors with a spontaneous ruthenium atomic moment, e.g., $Y_2Ru_2O_7$. While there have been a number of attempts to correlate the structural and electronic properties of the ruthenate pyrochlores (3–5, 11–13) only for a handful of these materials are precise structural data available. For a number of these studies the interest has been directed toward understanding the ordering of the oxygen vacancies and the A site cation in the oxygen-deficient pyrochlores such as $Pb_2Ru_2O_{6.5}$ (6, 14). As described by Bweyerlein *et al.* (6), weak (420) and (640) reflections are observed in the X-ray diffraction pattern of $Pb_2Ru_2O_{6.5}$ which are forbidden in space group $Fd\bar{3}m$ and the structure has thus been described in space group $F\bar{4}3m$. For other Ru pyrochlores such as $Bi_2Ru_2O_{6.9}$ (3) or $Tl_2Ru_2O_{6.7}$ (15), the oxygen vacancies are statistically disordered on the 8b site and the materials adopt a regular pyrochlore structure with space group $Fd\bar{3}m$.

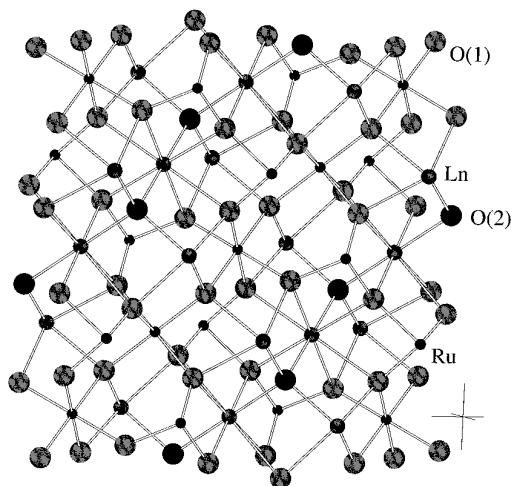


FIG. 1. Pyrochlore structure of general formula $A_2B_2O_6O'$ projected onto (1 1 0) showing the eightfold coordination of the A cations and sixfold coordination of the B cations. The O' atoms are only bonded to the A cations.

$Tl_2Ru_2O_{7-y}$ displays a metallic–semiconductor transition around 120 K, the exact temperature being dependent on the amount of oxygen vacancies (11). Kanno *et al.* (15) used powder neutron diffraction to determine the structure of both the stoichiometric, semiconducting material $Tl_2Ru_2O_7$ formed at low temperatures, hereafter referred to as Tl(LT), and the metallic oxygen-deficient material, $Tl_2Ru_2O_{6.7}$, formed at high temperatures, Tl(HT). Based on this and on previous powder X-ray diffraction studies, Kanno *et al.* concluded (15) that metallic ruthenate pyrochlores are characterized by relatively short Ru–O bonds, ca 1.95 Å compared with ca 1.98 Å in the semiconducting analogues, and more open Ru–O–Ru angles, 135–140° for metallic species versus 129–134° for semiconducting oxides. The effect of smaller Ru–O distances and larger Ru–O–Ru angles is to increase the overlap between the Ru 4*d* and O 2*p* orbitals. Independently an accurate neutron diffraction study of $Bi_2Ru_2O_7$ was reported by Facer *et al.* (3) in which the Ru–O distance was found to be 1.983 Å and the Ru–O–Ru angle 133.14°. Using the criteria of Kanno *et al.*, these data suggest that this metallic oxide should in fact be a semiconductor. There is an obvious need to further refine the ideas of Kanno *et al.* (15).

Recently Kennedy *et al.* (16) used powder neutron diffraction methods to determine accurate structural parameters in the series of stannate pyrochlores, $Ln_2Sn_2O_7$, and demonstrated that the Sn–O distance and Sn–O–Sn angles vary systematically with the size of the unit cell. Further for a given B site cation the lattice parameter of the pyrochlore is primarily determined by the ionic radii of the A site cation. These observations, together with the large

error in the oxygen positional parameter obtained by Kanno and co-workers in their powder X-ray structural study of $Bi_2Ru_2O_7$, 0.315(5) (5) versus 0.3266(1) found by Facer *et al.* (3) in their powder neutron diffraction study, prompted the present study in which neutron powder diffraction was used to accurately describe the structure of the four semiconducting ruthenate pyrochlores with $A = Nd, Pr, Tb$ and Yb . These compounds were selected to provide a wide range of lattice parameters and hence RuO_6 geometries. When taken with other published neutron diffraction studies, this work attempts to develop a more precise description of the structural differences between metallic and semiconducting ruthenate pyrochlores. A second aim of the present work is to identify periodic trends in the bonding of these complexes using valence bond sums.

EXPERIMENTAL

The ternary oxides $Ln_2Ru_2O_7$ were prepared by heating molar ratios of RuO_2 and M_2O_3 , Pr_6O_{11} , or Tb_4O_7 (Aldrich Chemicals 99.99%) in air. The materials were first mixed thoroughly in an agate mortar and cold pressed into 13-mm discs at 10 tons. The samples were heated progressively at 750, 850, and 1050°C for 24 h with intermediate regrindings. The materials were finally fired at 1200°C for 96 h. Powder X-ray diffraction measurements revealed the presence of small amounts of the orthorhombic fluorite related compounds Ln_3RuO_7 for $Ln = Pr, Nd,$ and Tb or Yb_2O_3 (17). This is presumably a consequence of loss of the more volatile Ru oxides.

The powder neutron diffraction data were collected using thermal neutrons with wavelength of 1.8857 Å on the high-resolution neutron powder diffractometer (HRNPD) at beamline H1A of the high-flux beam reactor (HFBR) at Brookhaven National Laboratory (BNL) (18, 19). The HRNPD is equipped with a bank of 64 individual 3He detectors, and data were collected at room temperature between 10° and 155° in 0.05° steps. About 5 g of the sample was housed in a thin walled vanadium container. No precautions to avoid preferred orientation were taken.

All structural refinements were performed using a version of Hill and Howard's program LHPM (20), modified for a personal computer. A Voigt function was used to model the shape of the peaks. The width of the Gaussian component was taken to vary in accordance with the expression due to Caglioti *et al.* (21), and the width of the Lorentzian component was coded to vary with $\eta \sec \theta$ to model particle size broadening. Since trace amounts, 2–4 wt%, of Ln_3RuO_7 (17) or Yb_2O_3 (22) were observed in the samples, the presence of this second phase was included in Rietveld refinement.

Valence bond sums and Madelung site potentials were calculated using the program EUTAX (23).

RESULTS AND DISCUSSION

The results of the neutron powder data refinement are presented in Table 1 and the fits to the powder patterns are shown in Fig. 2. The initial parameters of the impurity phases Pr_3RuO_7 , Nd_3RuO_7 , and Yb_2O_3 were taken from the literature (17, 22), while those for Tb_3RuO_7 were estimated from the previous work of van Berkel and Ijdo (24). In all cases no evidence for deviation from the expected stoichiometry of the pyrochlore phases was observed. This is in marked contrast to the metallic conducting ruthenate pyrochlores, which invariably contain appreciable oxygen vacancies. The individual bond lengths and angles of the pyrochlore phases are listed in Table 2.

Figure 3 shows a plot of the dependence of the cubic lattice parameter a_0 on the ionic radii of the A site cation r_A^{3+} for the 8 ruthenate pyrochlores $A_2\text{Ru}_2\text{O}_{7-y}$, $A = \text{Pr}$, Nd , Y , Tb , Bi , $\text{Tl}(\text{LT})$, and $\text{Tl}(\text{HT})$, the structures of which have been determined using powder neutron diffraction (3, 15, 25). It is immediately apparent from this figure that while the lattice parameter of the semiconducting Ln and Y pyrochlores display the expected simple linear response on r_A^{3+} for the three compounds containing group 13 or 15 cations, Tl or Bi on the A site, there is considerable deviation from this simple relationship. For the Bi compound this is a negative deviation; the lattice parameter is smaller than anticipated and for the Tl samples there is a positive deviation, the lattice parameter being larger than predicted. The anomalous behavior of the three group 13/15 compounds is further illustrated in Fig. 4, where the unique oxygen positional parameter is seen to be systematically lower than the values observed for the Ln or Y compounds, which display a linear decrease in x as the lattice parameter increases. Ideally the structure of a ruthenate pyrochlore with a lattice parameter in the range 10.20–10.30 Å should be studied by neutron diffraction methods; however, the cations which yield such values, Sm , Eu , and

Gd , all have prohibitively high neutron absorption cross sections. It should be noted that even for the semiconducting materials, the observed values for x are at best in poor agreement with those predicted using the mathematical relationship developed by Nikiforov (26) and exploited by McCauley (27), implicating that electronic effects are equally important in controlling the value of x .

For the pyrochlore structure, the sixfold coordination of the B site cation, Ru , is a trigonal antiprism stretched along the -3 axis so that the distance between two oxygen ions of opposite basal planes is larger than the distance between two oxygen ions in the same basal plane. For a given lattice parameter, as the value of x decreases, the $\text{Ru}-\text{O}$ distance decreases and the trigonal antiprism is compressed along the -3 axis until at $x = 0.3125$ a regular octahedron is obtained. At the same time the decrease in x lessens the apparent compression in the AO_8 scalehedron, the two $\text{A}-\text{O}(2)$ bonds along the -3 axis are noticeably shorter than the other six, equidistant, $\text{A}-\text{O}(1)$ distances (Table 2). Since the short $\text{A}-\text{O}$ distance is to $\text{O}(2)$ and this distance is independent of the x value, what in fact happens is that the $\text{A}-\text{O}(1)$ distance decreases more rapidly as x increases. Thus it would appear that the polarizable A site cations, Tl and Bi , repel the distant $\text{O}(1)$ atom, causing the RuO_6 polyhedron to become more compressed and the $\text{Ru}-\text{O}$ bond distances to shorten. This effect is illustrated in Fig. 5, where the $\text{Ru}-\text{O}$ and $\text{A}-\text{O}(1)$ bond distances are seen to be anomalous for the group 13/15 cations containing compounds, although this effect is extremely subtle and only becomes evident on examination of a number of structures.

A second structural consequence of the variation in the oxygen positional parameter is the variation in the $\text{Ru}-\text{O}-\text{Ru}$ angle. As discussed in more detail elsewhere by Kanno and co-workers (4, 5, 15), it is generally believed that metallic conductivity in the ruthenate pyrochlores requires an "opening-up" of the $\text{Ru}-\text{O}-\text{Ru}$ angle. This indeed appears to be the case, as is revealed in Fig. 6, where a number of other metallic ruthenates have been included for comparison. There is a clear difference between the Ln or Y ruthenates and those with group 13/15 cations, where in all cases the $\text{Ru}-\text{O}-\text{Ru}$ angle is considerably greater than expected purely on the basis of the size of the A site cation. In light of the present data, the bond angles of the two Tl compounds appear the most unusual and suggest that if the $\text{Ru}-\text{O}-\text{Ru}$ angle is less than 133° the compound will be a semiconductor and if it is greater than 133° it will be a metallic oxide provided the $\text{Ru}-\text{O}$ distance is acceptably small. Overall, however, it is obvious from Fig. 5 and 6 that the structural differences between the metallic and semiconducting ruthenate pyrochlores are extremely small.

The above describes the essential structural differences between the metallic and semiconducting ruthenate pyro-

TABLE 1
Structural and Isotropic Thermal ($\times 10^{-3}$ Å) Parameters for $Ln_2\text{Ru}_2\text{O}_7$ Pyrochlores

	Pr	Nd	Tb	Yb
Ionic radii (Å) ²⁸	1.126	1.109	1.040	0.985
a (Å)	10.3775(1)	10.3442(1)	10.2063(1)	10.0752(2)
x	0.3295(1)	0.3301(2)	0.3353(2)	0.3378(2)
B_{iso}				
Ln	0.64(3)	0.86(5)	0.64(5)	0.87(5)
Ru	0.44(3)	0.20(4)	0.40(4)	0.76(3)
$\text{O}(1)$	0.47(1)	0.50(3)	0.62(3)	0.95(2)
$\text{O}(2)$	0.58(3)	0.69(10)	-0.14(9)	0.24(11)
R_p^{20}	6.62	7.24	6.99	7.52
R_{wp}	8.94	9.90	8.95	10.62
R_{exp}	3.34	3.59	3.59	5.16
R_{Bragg}	2.44	2.21	3.23	2.60

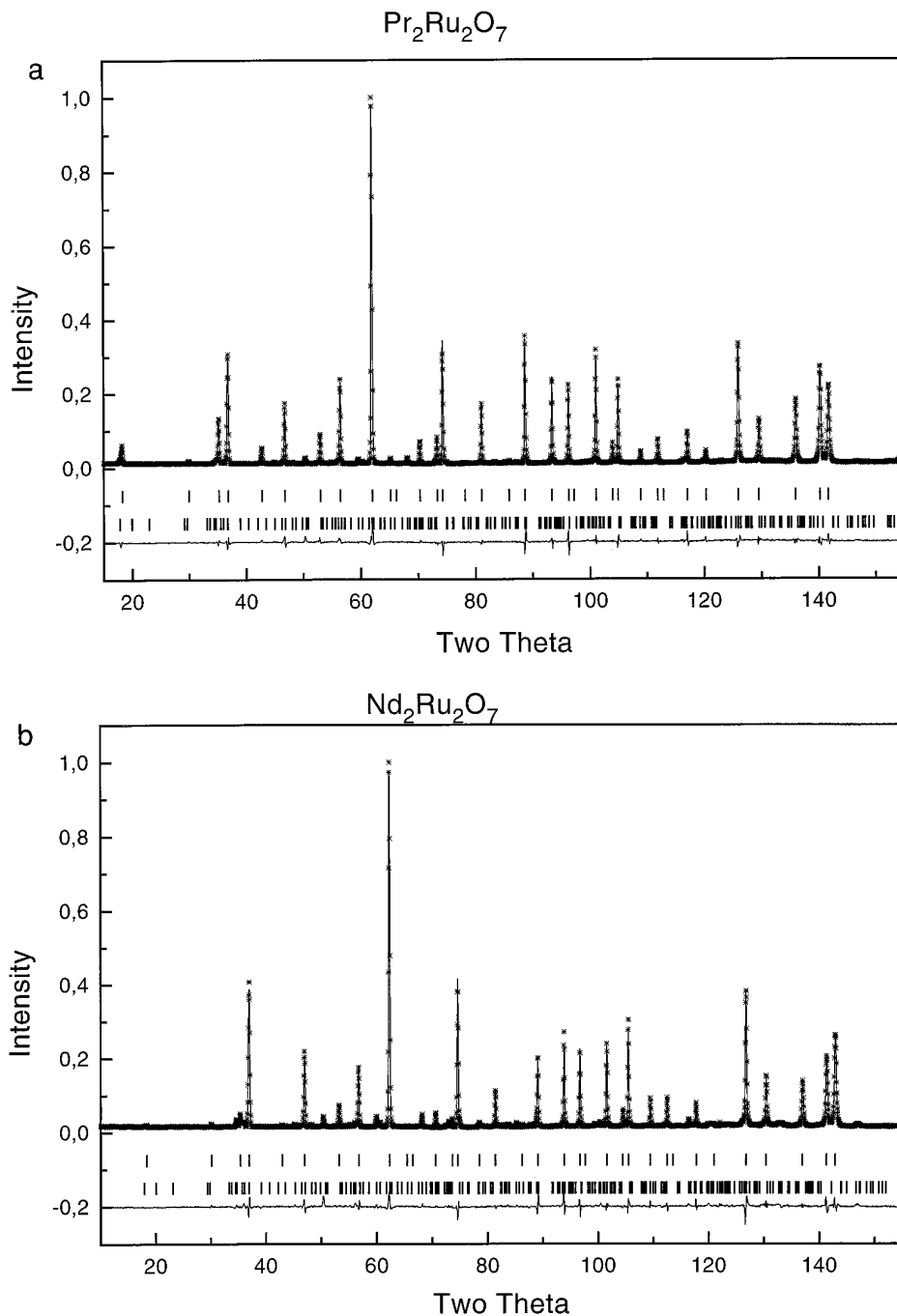


FIG. 2. Rietveld refinement plot of (a) $\text{Pr}_2\text{Ru}_2\text{O}_7$, (b) $\text{Nd}_2\text{Ru}_2\text{O}_7$, (c) $\text{Tb}_2\text{Ru}_2\text{O}_7$, and (d) $\text{Yb}_2\text{Ru}_2\text{O}_7$. The upper tick marks indicate the location of individual Bragg reflections due to the pyrochlore phase and the lower tick marks those of impurity phases. The lower curve is the difference plot between the observed and calculated profiles.

chlores, namely the relatively large Ru–O–Ru angle and short Ru–O bond distances. However, this still does not answer the question of why the lattice parameters of the Bi and Tl compounds are anomalous. As may be expected, part of the answer is related to the structural requirements of good conductivity. If the Bi compound were to have a

normal “lattice parameter,” a value of 10.479 \AA could be extrapolated from the series of five *Ln* and Y pyrochlores. Then a “favorable” Ru–O–Ru angle, $>133^\circ$, is found for any value of $x < 0.3242$, a value also obtained by extrapolation of the *Ln* data. However, this results in longer Ru–O bonds, 2.019 \AA , unless the value of x is decreased. In order

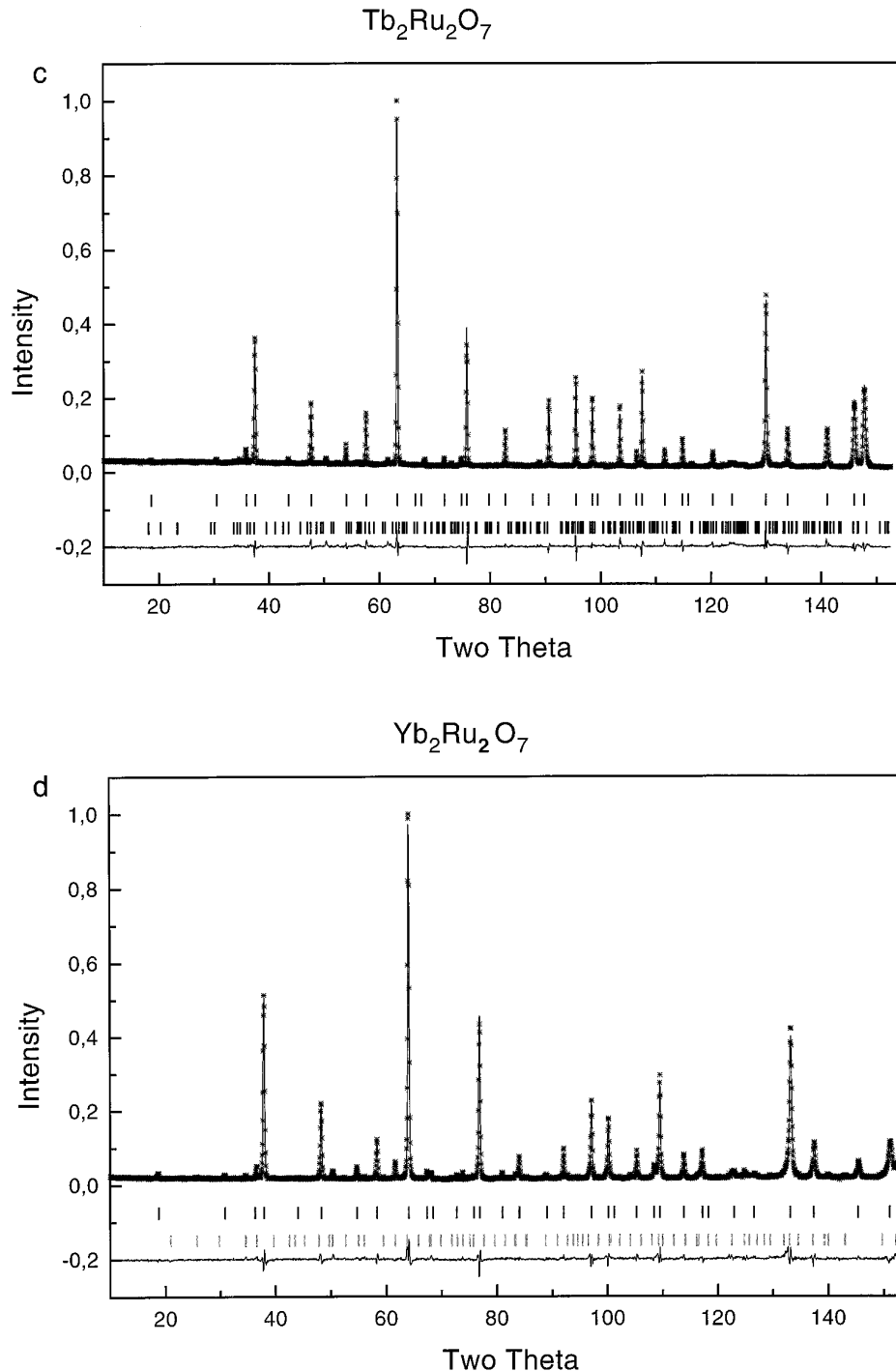


FIG. 2—Continued

for the Bi compound to have both reasonably short Ru–O bond distances and a large Ru–O–Ru angle it is necessary for the lattice to contract below the predicted value. In the case of the Tl compounds, the extrapolated lattice and oxygen positional parameters provide a “favorable” Ru–O distance, 1.976 Å; however, the Ru–O–Ru angle is unac-

ceptably small for metallic conductivity. In order to obtain favorable Ru–O overlap, the value of x needs to be reduced toward the observed value. At the same time, unless the lattice expands, this would result in an unacceptably short Ru–O bond distance of 1.93 Å, which is significantly shorter than the sum of the ionic radii for Ru^{4+} , 0.62 Å, and

TABLE 2
Selected Structural Features for $A_2Ru_2O_7$ Compounds

	$Bi_2Ru_2O_7$	$BiCaRu_2O_7$	$PbNdRu_2O_7$	$Tl_2Ru_2O_7$ (HT)	$Tl_2Ru_2O_7$ (LT)	$Pr_2Ru_2O_7$	$Nd_2Ru_2O_7$	$Tb_2Ru_2O_7$	$Y_2Ru_2O_7$	$Yb_2Ru_2O_7$
a (Å)	10.2957	10.2246	10.2978	10.2008	10.2116	10.3775	10.3442	10.2063	10.1429	10.0752
x	0.3266	0.3256	0.3251	0.3235	0.3273	0.3295	0.3301	0.3353	0.33527	0.3378
y	0.08	0.14	0.19	0.29	0.00	0.00	0.00	0.00	0.00	0.00
Metallic	Yes	Yes	Yes	Yes	No	No	No	No	No	No
$B-O$	1.984	1.966	1.978	1.953	1.970	2.012	2.008	1.999	1.991	1.989
$6 \times A-O(1)$	2.550	2.539	2.561	2.549	2.523	2.549	2.536	2.459	2.450	2.417
$2 \times A-O(2)$	2.229	2.214	2.230	2.209	2.211	2.247	2.240	2.204	2.196	2.181
$B-O-B$	133.14	133.69	133.97	134.88	132.74	131.57	131.25	128.48	128.45	127.18
Ref.	3	14	5	15	15	This work	This work	This work	25	This work

O^{2-} , 1.38 Å (28). Thus in order to obtain large Ru–O–Ru angles, and an acceptably short Ru–O bond distance there is the need for appreciable variation in the lattice parameters. This point will be discussed further below.

The presence of easily polarizable group 13/15 cations apparently enhances the opening of the Ru–O–Ru contact to the point where the Ru 4d electrons are near the transition from itinerant to localized behavior (11–13). This raises the question of what the electronic implications of these structural changes are. To address this, valence bond sums and Madelung site potentials have been calculated using the program EUTAX (23). The valence sums are obtained by first determining bond valencies as

$$\nu_{ij} = \exp[(R_0 - d_{ij})/0.37 \text{ \AA}],$$

where values for R_0 are the valence bond parameters for each bond pair and d_{ij} are the actual bond distances. The values of R_0 were taken from the literature (29). Valence bond sums were then obtained by simply summing over all neighbors for each site:

$$V_i = \sum \nu_{ij}.$$

Figure 7 illustrates the variation in the valence bond sums for the four types of atoms in the cell: A, Ru, O(1), and O'. For the Bi and Tl compounds, the Ru valence bond sums are larger and the A site values are lower than would be anticipated from comparison with the Ln or Y compounds. Even for the "simple" semiconducting ruthenates, the band valence calculations deviate significantly

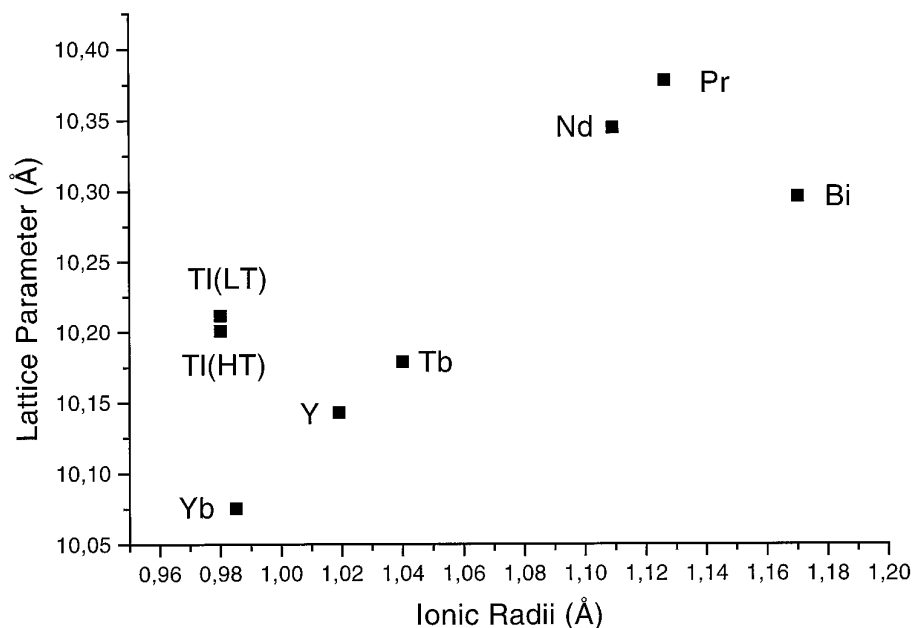


FIG. 3. Cubic lattice parameter as a function of the ionic radii of the A site cation for some ruthenium pyrochlores. The data for the nonmetallic lanthanide containing oxides follow an apparent linear variation.

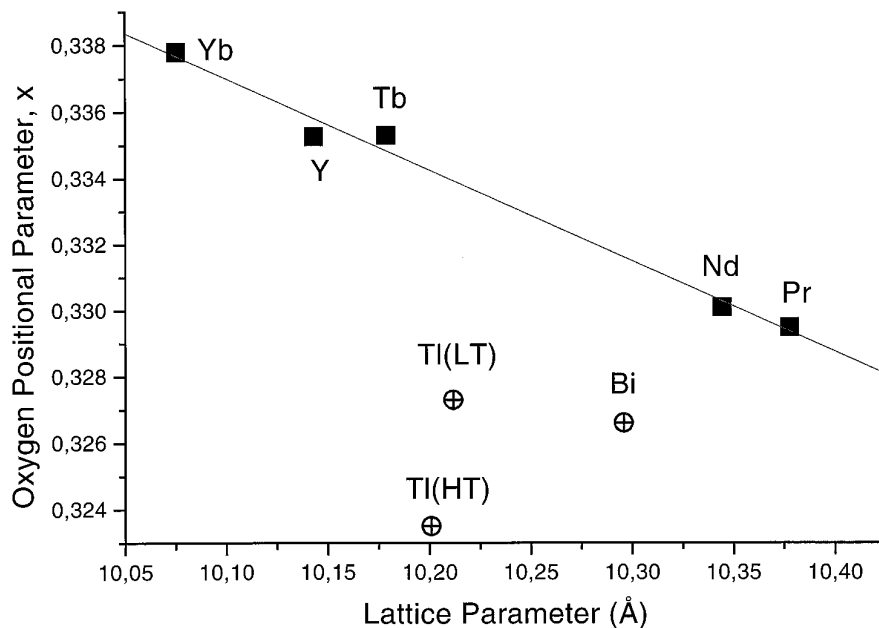


FIG. 4. Oxygen positional parameter, x , as a function of the cubic lattice parameter for some ruthenium pyrochlores. The data for the nonmetallic lanthanide containing oxides follow an apparent linear variation.

from the formal valence charges. The variation in valence bond sums from the formal charge on the ion is generally ascribed to either strain in the bonding or covalency (30) and has, for example, been observed by Fourquet *et al.*

(31) in the pyrochlore $Tl_2Nb_2O_{6+x}$, where covalent interactions are believed to be important. The present results indicate a decrease in the electron density (increased valence) of the Ru centers and a concurrent increased density

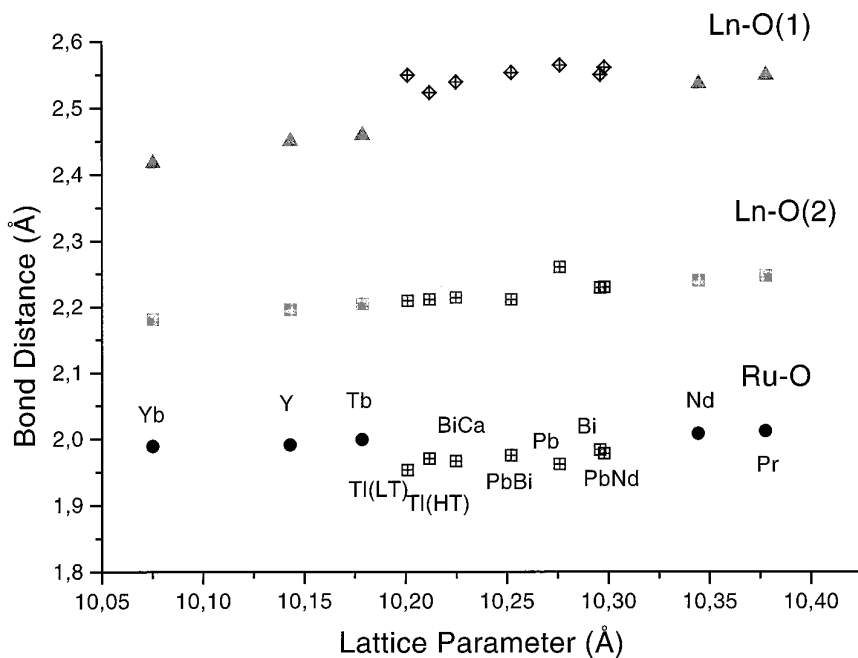


FIG. 5. Ru-O and Ln-O bond distances as a function of the cubic lattice parameter for some ruthenium pyrochlores. The data for the nonmetallic lanthanide containing oxides follow an apparent linear variation.

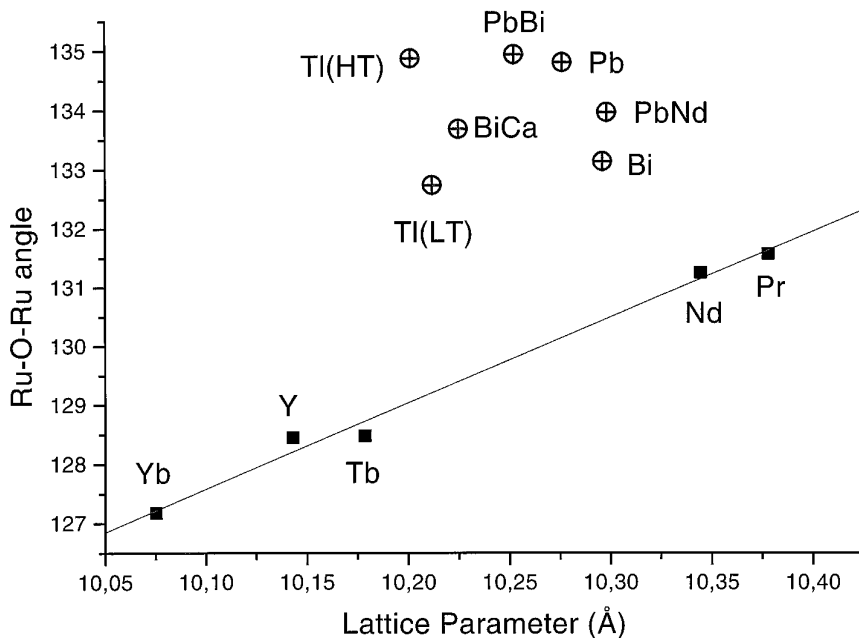


FIG. 6. Ru-O-Ru angle as a function of the cubic lattice parameter for some ruthenium pyrochlores. The data for the nonmetallic lanthanide containing oxides follow an apparent linear variation.

in the Tl and Bi cation relative to the more normal semiconductors. For the Tl compounds, at least, this is readily explained by allowing for partial reduction of the formal Tl^{3+} ions to Tl^+ , which would cause an increase in the effective ionic radii of the *A* site cation and thus an increase in the lattice parameter as is in fact observed. This is also in agreement with the appreciable oxygen vacancies observed in $Tl_2Ru_2O_{7-y}$ (15). There is evidence to suggest that both oxidation states of Tl can coexist in the oxygen defect pyrochlores Tl_2NbO_{6+x} and $Tl_2Ta_2O_6$ (32), although in these compounds the Tl is displaced away from the 16 *d* sites at (0.5, 0.5, 0.5) and is statistically distributed on half the 32(*e*) positions at (*u*, *u*, *u*), where $u \cong 0.5$ (31). As the oxygen content increases, the Tl moves toward the 16(*d*) site. There is no evidence to suggest a similar displacement has occurred in the ruthenate pyrochlores. Nevertheless there does appear to be a partial reduction of the Tl^{3+} . In principle this can be compensated for by oxidation of some of the formal Ru^{4+} to Ru^{5+} and/or the formation of oxygen vacancies. In metallic Tl(HT), the latter occurs. Since the ionic radii of Ru^{4+} and Ru^{5+} are reasonably similar, the former mechanism would have little influence on the cubic lattice parameter but could lead to shorter Ru-O bond distances, as is indeed observed in Fig. 6. Structurally it is not possible to estimate the amount of Ru^{5+} present. In principle it should be possible to estimate the amount of Ru^{5+} present using photoelectron spectroscopy; however, strong final state effects in the metallic ruthenates preclude this (3, 13).

For $Bi_2Ru_2O_{7-y}$ the explanation is a little more problem-

atic since the lattice parameter has apparently contracted while the "effective" oxidation state of the Bi has decreased.¹ The decrease in the effective Bi oxidation state agrees with the presence of appreciable oxygen vacancies on the O(2) site. However, it is difficult to imagine formal reduction of the Bi^{3+} occurring; intuitively partial reduction of the Ru^{4+} is expected to occur to compensate for the oxygen vacancies and indeed electrochemical measurements demonstrate that Ru^{3+} is formed before bulk reduction of Bi^{3+} occurs (7, 33). Reduction of Ru^{4+} is, however, expected to slightly increase the lattice parameter in contrast to the behavior shown in Fig. 3. It must, however, be recalled that Bi^{3+} has a 6*s* lone pair (as does Tl^+) which can be stereochemically active. Initially the 6*s* lone pair is thought to be uniformly delocalized around the Bi^{3+} center; however, it is feasible that these electrons are involved in strong covalent interactions with the Bi-O(2) bond, resulting in a contraction in the BiO_8 scalehedron and hence in the cubic lattice parameter. Indirect evidence for such an explanation comes from two sources. First, a maximum entropy electron density study of $Y_2Sn_2O_7$ has been performed which suggests that there is weak Y-O covalency (34). Second, the six long Bi-O bond distances in $Bi_2Ru_2O_{7-y}$, 2.576 Å, are significantly longer than found

¹ As pointed out by Shannon (28), there is some uncertainty on the precise effective ionic radii of Bi^{3+} ions in the pyrochlore lattice. We have utilized the value deduced by Shannon for a dormant lone pair of 1.17 Å—a value closer to 1.08 Å would be required for $Bi_2Ru_2O_7$ to appear as a "normal" pyrochlore in Fig. 3.

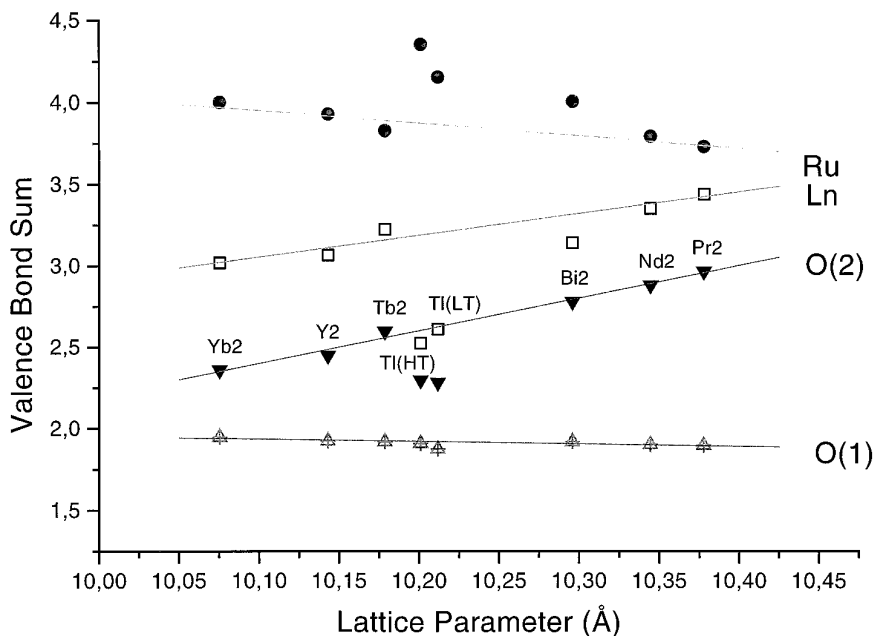


FIG. 7. Valence bond sums as a function of the cubic lattice parameter for some ruthenium pyrochlores.

in other compressed BiO_8 scalehedra; for example, in $\text{Bi}_3\text{Ru}_3\text{O}_{11}$ the corresponding distance is 2.478 Å, while in the insulating oxide $\text{Bi}_3\text{Sb}_2\text{AlO}_{11}$ the distance is 2.504 Å. Unfortunately no precise structural data are yet available for a nonmetallic pyrochlore with only Bi^{3+} ions in the *A* site. A more systematic study of the possible role of the Bi lone pair is required.

CONCLUSION

The present work has provided accurate and precise structural parameters for a number of semiconducting ruthenate pyrochlores, thus enabling a detailed study of the structural features in metallic versus semiconducting ruthenate pyrochlores. While the differences in the Ru–O bond distances between the two systems are small, these results highlight the importance of the easily polarizable group 13/15 cations in allowing large Ru–O–Ru angles. In the pyrochlores, Ru–O–Ru angles greater than 133° are undoubtedly necessary to have metallic conductivity. However, it appears that electron delocalization from the *A* site cation is at least equally important. A recurring theme in the structural chemistry of the metallic ruthenate pyrochlores is the presence of appreciable vacancies at the *8b* oxygen site. These oxygen atoms are not part of the RuO_6 polyhedra and it is possible that partial formal oxidation to Ru(V) occurs via electron transfer from the *A* site cation despite their presence. The importance of these vacancies has yet to be quantified.

ACKNOWLEDGMENTS

We gratefully acknowledge support of this work by the Australian Research Council and, at Brookhaven National Laboratory, under Contract DE-AC02-76CH00016, the Division of Materials Sciences, US Department of Energy. B.J.K. also thanks ANSTO for the provision of a travel grant.

REFERENCES

1. H. von Gaertner, *Neues Jahrb. Mineral. Geol. Palaeontol. Ref.* **61**, 1 (1930).
2. M. A. Subramanian, G. Aravamudan, and G. V. Subba Rao, *Progr. Solid State Chem.* **15**, 55 (1983).
3. G. Facer, M. M. Elcombe, and B. J. Kennedy, *Aust. J. Chem.* **46**, 1897 (1993).
4. R. Kanno, Y. Takeda, T. Yamamoto, Y. Kawamoto, and O. Yamamoto, *J. Solid State Chem.* **102**, 106 (1993).
5. H. Kobayashi, R. Kanno, Y. Kawamoto, T. Kamiyama, F. Izumi, and A. W. Sleight, *J. Solid State Chem.* **114**, 15 (1995).
6. R. A. Beyerlein, H. S. Horowitz, J. M. Longo, and M. E. Leonowicz, *J. Solid State Chem.* **51**, 253 (1984).
7. R. G. Edgell, J. B. Goodenough, A. Hamnett, and C. C. Naish, *J. Chem. Soc. Faraday Trans. I* **79**, 893 (1983).
8. H. S. Horowitz, J. M. Longo, H. H. Horowitz, and J. T. Lewandowski, *ACS Symp. Ser.* **127**, 143 (1985).
9. T. R. Felthouse, P. B. Fraundorf, R. M. Friedman, and C. L. Schosser, *J. Catal.* **127**, 421 (1991).
10. P. F. Carcia, A. Ferreti, and A. Suna, *J. Appl. Phys.* **53**, 5282 (1982).
11. H. S. Jarrett, A. W. Sleight, J. F. Weiher, J. L. Gillson, C. G. Frederick, G. A. Jones, R. S. Swingle, D. Swatzfager, J. E. Gulley, and P. C. Hoell, in "Valence Instabilities and Related Narrow Band Phenomena" (R. D. Parks, Ed.), p. 545, Plenum Press, New York, 1977.
12. W. Y. Hsu, R. V. Kasowski, T. Miller, and T. C. Chiang, *Appl. Phys. Lett.* **52**, 7 (1988).

13. P. A. Cox, J. B. Goodenough, P. J. Tavener, D. Telles, and R. G. Edgell, *J. Solid State Chem.* **62**, 360 (1986).
14. B. J. Kennedy, *J. Solid State Chem.* **119**, (1995) 254.
15. R. Kanno, J. Huang, and A. W. Sleight, in "Proceedings of the Fifth International Symposium on Advanced Nuclear Energy Research," P-127, 1994.
16. B. J. Kennedy, C. J. Howard, and B. A. Hunter, in preparation.
17. W. A. Groen, F. P. F. van Berkel, and D. J. W. Ijdo, *Acta Crystallogr. Sect. C* **43**, 2262 (1987).
18. T. Vogt, L. Passell, S. Cheung, and J. D. Axe, *Nucl. Instrum. Methods A* **338**, 71 (1994).
19. J. D. Axe, S. Cheung, D. E. Cox, L. Passell, and T. Vogt, *J. Neutron Res.* **2**, 85 (1994).
20. R. J. Hill and C. J. Howard, "Australian Atomic Energy Commission Report No. M112, "AAEC (now ANSTO), Lucas Heights Research Laboratories, New South Wales, Australia, 1986.
21. G. Caglioti, A. Paoletti and F. P. Ricci, *Nucl. Instrum.* **3**, 223 (1958).
22. T. Schleid and G. Meyer, *J. Less Common Metals* **149**, 73 (1989).
23. M. O'Keeffe, "EUTAX, Version 1.3" EMLab Software, Phoenix, AZ, 1993.
24. F. P. F. van Berkel and D. J. W. Ijdo, *Mater. Res. Bull.* **21**, 1103 (1986).
25. B. J. Kennedy, *Acta Crystallogr. Sect. C* **51**, 790 (1995).
26. L. G. Nikiforov, *Sov. Phys. Crystallogr. B* **5**, 925 (1969).
27. R. A. McCauley, *J. Appl. Phys.* **51**, 290 (1980).
28. R. D. Shannon, *Acta Crystallogr. Sect. A* **32**, 751 (1976).
29. I. D. Brown and D. Altermatt, *Acta Crystallogr. Sect. B* **41**, 244 (1985).
30. I. D. Brown, *Acta Crystallogr. Sect. B* **48**, 553 (1992).
31. J. L. Fourquet, H. Duroy, and Ph. Lacorre, *J. Solid State Chem.* **114**, 575 (1995).
32. M. Ganne and M. Tournoux, *Mater. Res. Bull.* **10**, 1313 (1988).
33. G. Gokagac and B. J. Kennedy, *J. Electroanal. Chem.* **368**, 235 (1994).
34. M. Takata, B. J. Kennedy, and C. J. Howard, unpublished observations.